Journal of Colloid and Interface Science xxx (2012) xxx–xxx

Contents lists available at SciVerse ScienceDirect

Journal of Colloid and Interface Science

www.elsevier.com/locate/jcis

A three parameter description of the structure of diffusion limited cluster fractal aggregates

W.R. Heinson, C.M. Sorensen *, A. Chakrabarti

Department of Physics, Kansas State University, Manhattan, KS 66503, United States

ARTICLE INFO

Article history:
Received 29 November 2011
Accepted 31 January 2012
Available online xxxx

Keywords:
Fractal aggregates
Fractal dimension
Diffusion limited cluster aggregation (DLCA)
Aggregates
Morphology
Agglomerates
Pair correlation function
Structure factor
Packing fraction
Anisotropy

ABSTRACT

A three parameter description of fractal aggregates is derived from the pair correlation function of the monomeric units that compose the aggregate. The parameters describe the mass fractal scaling with linear size (the fractal dimension), the packing fraction density of the spherical monomers, and the overall shape of the aggregates. Values for these three parameters are determined for diffusion limited cluster aggregates (DLCAs) in three dimensions. The effects of these parameters are found in terms of measureable quantities in both real and reciprocal space.

1. Introduction

When solid particles come together via random aggregation processes, they form aggregates with a self similar, fractal morphology [1–3]. Typically, aggregation in aerosols and colloids involves clusters hitting and sticking to other clusters, so called cluster–cluster aggregation. The motion between the collisions is most commonly diffusive to yield diffusion limited cluster–cluster aggregation, DLCA. Variants exist including ballistic motion between collision (BLCA), which can occur in aerosols, and reaction limited aggregation (RLCA), which can occur in colloids.

A fractal aggregate is a cluster of primary particles (or monomers) that has a self-similar structure between the scale of the monomers and the overall size of the aggregate. Ideally the monomers are same-sized spheres of radius a with point contacts. The overall size is well described by the radius of gyration R_g which is a root mean square radius. A consequence of self-similarity is power law functionalities; hence the number of monomers N in the aggregate, which is proportional to the aggregate mass, scales as a power law with the reduced size of the aggregate as

$$N = k_0(R_g/a)^{D_f} \quad (1)$$

In Eq. (1) D_f is the fractal dimension and k_0 is the scaling prefactor. Eq. (1) may be considered as the defining relation for fractal aggregates (see, for example, Ref. [4]). For DLCA simulations, values near $D_f = 1.8$ and $k_0 = 1.35$ have been found in numerous studies [5–9].

Eq. (1) has great utility in describing the morphology of fractal aggregates. However, it is by no means comprehensive. An important feature not described by Eq. (1) is shape [10,11]. In recent work we addressed the issue of shape for DLCA aggregates [12]. We found that the fractal dimension was independent of shape, but the prefactor was strongly dependent. This dependence can be understood by using Eq. (1). For a given N, as the cluster becomes more non-spherical, the radius of gyration increases, and then by (1) k_0 must decrease. This work emphasized the importance of using both the fractal dimension and the prefactor to describe a given aggregate.

Despite the success of Eq. (1) in describing both the fractal nature and the shape of an aggregate, it is limited in that it ignores the structure of the aggregate at its smallest level, that of the monomer. In this paper we take what we will call a "bottom up approach" to the fractal aggregate structure by starting with the manner in which spherical monomers can pack in space. From this the monomer pair correlation function is derived. After that, an analytical formalism developed by Nicolai et al. [13] is followed to find relationships between the fractal dimension, prefactor, shape and monomer packing. Results of DLCA simulations are then described to test these relationships yielding quantitative values

* Corresponding author.
E-mail address: sor@phys.ksu.edu (C.M. Sorensen).

0021-9797/$ - see front matter © 2012 Elsevier Inc. All rights reserved.
doi:10.1016/j.jcis.2012.01.062

for their magnitudes. Our results extend those of Nicolai et al. [13] by quantifying their parameter r_0^* in terms of a volume packing fraction, see Eq. (4) below, and relating the stretching exponent γ of the pair correlation function, see Eq. (9) below, to the aggregate anisotropy. We also show how these parameters affect the aggregate structure factor. We achieve a new, three parameter description of fractal aggregates that connects the monomeric length scale to the overall aggregate length scale.

2. Theory

The bottom up approach starts with the packing of spheres in space. The number of spherical monomers of radius a and volume v_0 in a volume of radius r of volume $V(r)$ is

$$N(r) = \varphi \frac{V(r)}{v_0} = \varphi \left(\frac{r}{a}\right)^3 \tag{2}$$

where φ is the packing fraction. For fractals, where the dimensionality is $D_f \neq 3$, we generalize this formulation to

$$N(r) = \varphi \left(\frac{r}{a}\right)^{D_f} = \left(\frac{r}{r_0^*}\right)^{D_f} \tag{3}$$

This equation defines a rescaled monomer radius in the notation of Nicolai et al. [13]

$$r_0^* = \varphi^{-1/D_f} a \tag{4}$$

The monomer pair correlation function is the probability that another monomer center will be found a distance r from a given monomer center. In *isotropic* systems the correlation function $g(r)$ is constrained by the normalization condition

$$\int \rho g(r) 4\pi r^2 dr = N \tag{5}$$

where ρ is a *constant* density. In fractals, however, ρ is a function of r. One thus writes a *working* definition of $g(r)$ as proportional to the average number of monomers in a shell of radius r and thickness dr.

$$g(r) \approx \left\langle \frac{\text{monomers in } dV}{4\pi r^2 dr} \right\rangle \tag{6}$$

Consequently the normalization becomes

$$\int g(r) 4\pi r^2 dr = N \tag{7}$$

With this working definition of $g(r)$ and with the self-similar nature of fractal aggregates, the monomer from which the pair correlation function is measured is completely arbitrary. The structure around each monomer will be on average the same so Eq. (6) is an ensemble average. With Eqs. (3) and (6) and the proper normalization, the pair-correlation is

$$g(r) = \frac{dN}{4\pi r^2 dr} = \frac{D_f}{4\pi r_0^{*D_f}} r^{D_f - 3} \tag{8}$$

Eq. (8) applies for clusters of infinite size, but for finite sizes the pair correlation function must have some cutoff function. It has become customary to assume a stretched exponential, which we will use here, to modify Eq. (8) to

$$g(r) = \frac{\varphi D_f}{4\pi a^{D_f}} r^{D_f - 3} \exp[-(r/\xi)^\gamma] \tag{9}$$

Eq. (9) introduces the stretching exponent γ and is consistent with Nicolai, Durand and Gimel except that we remove the rescaled monomer radius in favor of the actual monomer radius and the packing fraction. It is important to note that beyond the two length scales a and ξ, the pair correlation function is specified by three parameters, D_f, φ and γ.

The length scale ξ in the stretched exponential takes into account the finite size of the cluster. The stretched exponential implies an assumed spherical symmetry. The stretching exponent γ is a measure of how sharply the pair correlation cuts off at ξ; an infinite γ represents a sharp boundary. Real aggregates have diffuse boundaries and are not spherically symmetric. It is important to realize that the $g(r)$ for a non-spherical object with a sharp boundary, a rugby ball for example, when rotationally averaged would appear to have a diffuse boundary hence have a cutoff function with a finite γ. This would also be true for the ensemble averaged $g(r)$ for a set of rugby balls with random orientations. Thus it appears that the stretching exponent γ for an aggregate can have both an intrinsic source due to the diffuse nature of the surface and a source due to rotationally averaging. The later could be eliminated but at the expense of the additional complication of requiring a correlation function for all three spatial dimensions. We opt not to do this. Thus we anticipate that the stretching exponent γ will be related to shape anisotropy, a fact that will be demonstrated below.

The real space structure of the aggregate can now be calculated using

$$R_g^2 = \frac{2\pi}{N} \int g(r) r^4 dr \tag{10}$$

This yields Eq. (1) and a value for the prefactor of

$$k_0 = \left[\frac{2\Gamma(D_f/\gamma)}{\Gamma[(D_f+2)/\gamma]}\right]^{D_f/2} \frac{\varphi D_f \Gamma(D_f/\gamma)}{\gamma} \tag{11}$$

Eq. (11) shows that the prefactor is a function of three parameters, D_f, γ and φ.

The reciprocal space structure of the aggregate is described by the structure factor which is the Fourier transform of the pair correlation function and an important measurable quantity. For a spherically symmetric $g(r)$ the structure factor is given by

$$S(q) = \frac{P(q)}{N}\left[1 + 4\pi \int_0^\infty g(r) r^2 \frac{\sin(qr)}{qr} dr\right] \tag{12}$$

where $P(q)$ is the form factor of the monomer. In this work we will study the regime in which q^{-1} is large compared to the monomer radius, hence $P(q) = 1$. Substitution of (9) into (12) yields for large q

$$S(q) = \frac{b}{N}(q)^{-D_f}, \quad r_0^* \ll q^{-1} \ll \xi \tag{13}$$

where, in the notation of Nicolai et al. [13]

$$b = r_0^{*-D_f} D_f \Gamma(D_f - 1) \sin\left[\frac{\pi}{2}(D_f - 1)\right] \tag{14}$$

Eq. (13) has a $1/R_g$ dependence due to the limits $r_0^* \ll q^{-1} \ll \xi$. The characteristic size ξ is related to R_g by Eqs. (9) and (10). Eq. (13) does not collapse for fixed N but shifts on the x-axis based on $1/R_g$. Using a R_g normalization leaves only the gamma dependence of the $S(q)$ coefficient. Use of Eqs. (1), (4), and (14) in (13) yields

$$Sq = D_f \Gamma(D_f - 1) \sin\left(\frac{\pi}{2}(D_f - 1)\right) \varphi k_0^{-1} \left(q R_g^{-D_f}\right) \tag{15}$$

which will be useful below. Application of Eq. (11) yields

$$S(q) = \left[\frac{\Gamma(D_f - 1)}{\Gamma(D_f/\gamma)}\right]\left[\frac{\Gamma((D_f+2)/\gamma)}{2\Gamma(D_f/\gamma)}\right]^{D_f/2} \gamma \sin\left(\frac{\pi}{2}(D_f - 1)\right)(qR_g)^{-D_f} \tag{16}$$

Notice that structure factor has no φ dependence. The coefficient of the (qR_g) term depends only on D_f and γ the latter of which, as we will see, varies with the shape of the cluster.

Please cite this article in press as: W.R. Heinson et al., J. Colloid Interface Sci. (2012), doi:10.1016/j.jcis.2012.01.062

3. Simulation method

The work presented in this paper used an off-lattice diffusion limited cluster aggregation (DLCA) algorithm. Initially 10^6 monomers with radius a were randomly placed in a three dimensional box. The box size was determined so that the desired monomer volume fraction was obtained. Most of the results presented here are for $f_v = 0.001$, but several runs with a lower volume fraction $f_v = 0.0005$ were carried out to make sure that the results presented here belong to cluster dilute limit. At the beginning of each time step, the number of clusters (N_c) was counted (note that the number of monomers was included in N_c). A random cluster was chosen and time was incremented by N_c^{-1}. The probability that the cluster moved was inversely proportional to that cluster's radius of gyration ($p \propto R_g^{-1}$) and was normalized so that monomers had $p = 1$. Clusters moved in random directions a distance of one monomer diameter. When two clusters collided, they irreversibly stuck together, and N_c was decremented by 1. Simulations ran until 7000 clusters were left. Results are applicable in the continuum limit where the frictional drag is given by the Stokes–Einstein expression with a drag proportional to the radius of gyration.

4. Numerical calculations

A cluster's anisotropy and radius of gyration were found by diagonalizing the inertia tensor (T). For a three dimensional cluster made up of N monomers the inertia tensor is

$$T = \sum_{i-1}^{N} \begin{pmatrix} y_i^2 + z_i^2 & -x_i y_i & -x_i z_i \\ -x_i y_i & x_i^2 z_i^2 & -y_i z_i \\ -x_i z_i & -y_i z_i & x_i^2 y_i^2 \end{pmatrix} \xrightarrow{diagonalization} T = N \begin{pmatrix} R_1^2 & 0 & 0 \\ 0 & R_2^2 & 0 \\ 0 & 0 & R_3^2 \end{pmatrix} \tag{17}$$

The diagonalization of T yields principle radii $R_1 \geqslant R_2 \geqslant R_3$. Anisotropy is defined as

$$A_{13} = R_1^2 / R_3^2 \tag{18}$$

and is a measure of aggregate shape. The radius of gyration is a measure of overall size and is related to the principle radii by

$$R_g^2 = \frac{1}{2}\left(R_1^2 + R_2^2 + R_3^2\right) \tag{19}$$

Cluster pair correlation functions and structure factors were calculated. To calculate pair correlation a monomer in the cluster was chosen to be the center for shells of radius r and thickness dr progressing outward. For each shell the number of monomers was counted. These counts were divided by $4\pi r^2 dr$. The next monomer was then made the center for shells and monomers in those shells were counted again. This was done for all monomers in the cluster to obtain an ensemble average pair-correlation for the cluster. Structure factor for an aggregate was calculated from squaring the Fourier transform of the spatial coordinates of the monomers and normalizing by N^2 [4].

5. Results

The fractal dimension and prefactors of the ensembles of 7000 clusters were found in real space by finding the functionality of N versus R_g/a, Eq. (1). The results are shown in Fig. 1. The analysis looked at both all the aggregates and aggregates classified into groups of different anisotropy ranges, A_{13}. For each anisotropy range and all the aggregates an average R_g was found for every N. These groups were then averaged over four runs.

These results are quite consistent with our previous work [12] that showed that the fractal dimension is not dependent on the aggregate shape whereas the prefactor is strongly dependent. We conclude that the aggregates in these simulations are well described by $D_f = 1.80 \pm 0.02$ and $k_0 = 1.39 \pm 0.10$.

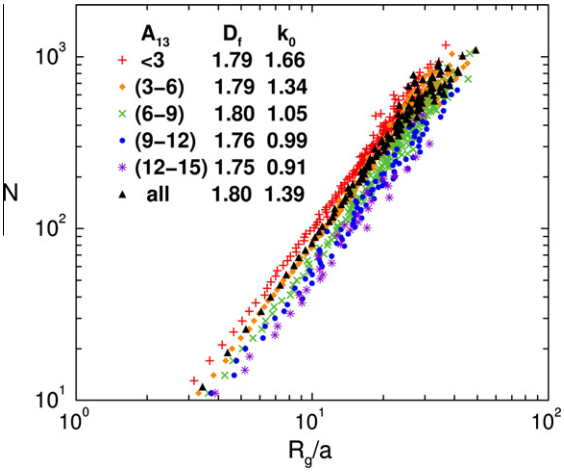

Fig. 1. Number of monomers versus normalized radius of gyration for all the aggregates and groups of aggregates classified by anisotropy, A_{13}.

Values for the packing fraction φ and stretching exponent γ were found by fitting the pair correlation function $g(r)$ of each individual aggregate to the analytical form of Eq. (9). The fit involved multiplication of $g(r)$ by r^{D_f-3}. Then the intercept of this form at $r = 0$ yields $D_f\,\varphi$. Two examples are shown in Fig. 2.

The small r limit of the pair correlation plots in Fig. 2 yields the product $D_f\,\varphi$. Taking $D_f = 1.80$, the limits from the fits to ca. 100 aggregates yield a packing fraction of $\varphi = 0.68 \pm 0.03$, independent of the shape of the aggregate. Also packing fraction was measured by application of Eq. (15) on the same ca. 100 aggregates and was found to be the same, within one percent, as the pair correlation packing fraction. This reinforces the concept that φ describes structure at the small aggregate length scales whereas A_{13} describes aggregate structure at large length scales. It is interesting to note that this packing fraction value is very close to the value found for random packing of spheres in three dimensions. It is also similar to a previously determined value in work where we attempted to understand packing of spheres in non-integer dimensionality spaces [7]. The corresponding value of r_0^*/a is found to be 1.24 ± 0.03.

The two examples of Fig. 2 also indicate that the shape, as quantified by the anisotropy parameter A_{13}, affects the stretching exponent γ. Analysis of ca. 100 aggregates yields the data in Fig. 3 which

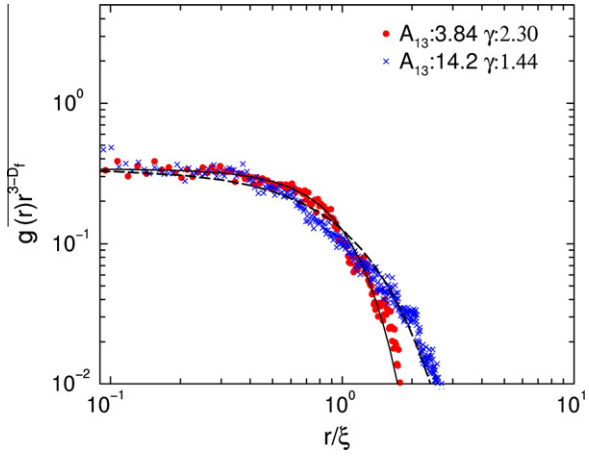

Fig. 2. Pair correlation function $g(r)$ of two $N = 500$ aggregates with fits from Eq. (9).

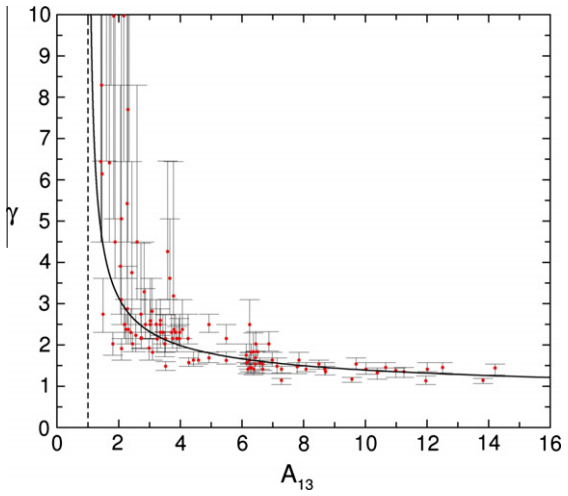

Fig. 3. The stretching exponent γ versus the anisotropy parameter A_{13}. Individual aggregates of $N \geqslant 500$ are plotted. Data points are individual DLCA aggregates. Error bars represent a range of gamma values for a given aggregate. The solid line is the combination of Eqs. (11) and (22). The dashed line represents spherical clusters with the lowest possible value of $A_{13} = 1$.

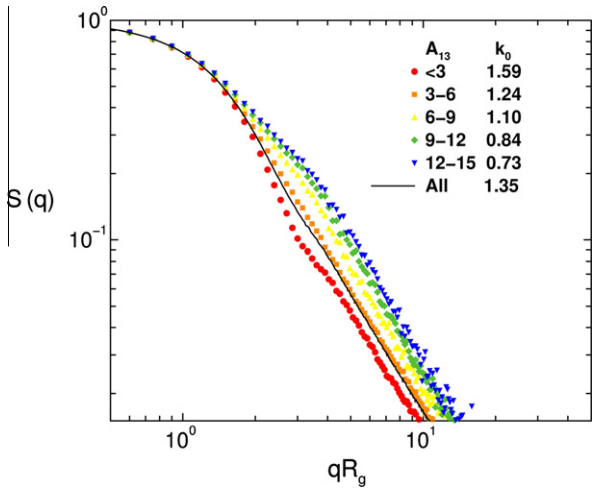

Fig. 5. Structure factors for all the aggregates and groups of aggregates classified by anisotropy, A_{13}. Structure factors were calculated from squaring the Fourier transform of the spatial coordinates of the monomers and normalizing by N^2. Aggregates were divided into groups according to A_{13} and structure factor for the clusters in each group were averaged.

shows γ as function of A_{13}. The concept that the stretching exponent would have both an intrinsic component, due to the aggregate surface structure, and a shape component, that appears upon rotationally averaging the aggregate, was anticipated above and is supported here.

With $\varphi = 0.68$ and $D_f = 1.8$, Eq. (11) provides a description of the how the prefactor k_0 changes with γ. This is tested against the simulation data in Fig. 4. The limit of Eq. (11) can be evaluated as

$$\lim_{\gamma\to\infty} k_0 = \varphi\left(2 + 4/D_f\right)^{D_f/2} \tag{20}$$

For $D_f = 1.8$ and $\varphi = 0.68$, $\lim_{\gamma\to\infty} k_0 = 2.48$. This limit is included in Fig. 4.

As mentioned above, our recent work showed that the prefactor k_0 was a function of shape anisotropy, as specified by A_{13}, whereas the fractal dimension was not [12]. Since A_{13} and γ are coupled together, Eqs. (15) and (16) show that the coefficient of the fractal

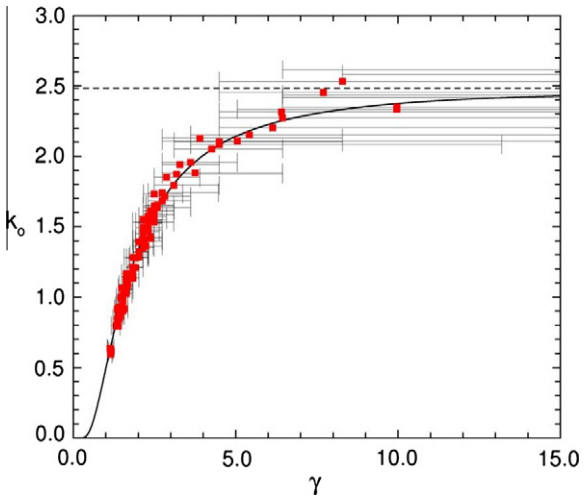

Fig. 4. The prefactor k_0 versus the stretching exponent γ. Data points are individual DLCA aggregates. Error bars represent a range of gamma values for a given aggregate. The solid line represents Eq. (11); the dashed line is the limit of Eq. (20), $\lim_{\gamma\to\infty} k_0 = 2.48$, both using $\varphi = 0.68$ and $D_f = 1.8$.

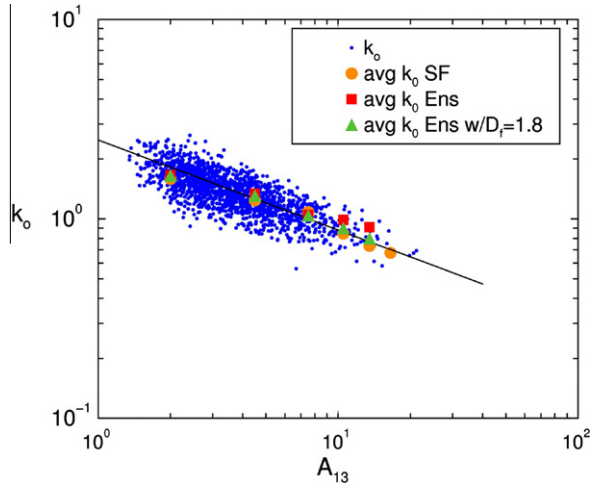

Fig. 6. Large circles are the k_0 values for different A_{13} groups from structure factor (SF). The large squares are k_0 values for different A_{13} groups from the N versus R_g data of Fig. 1 and triangles are the same data forced to $D_f = 1.8$. Small circles are k_0 versus A_{13} for individual clusters and follow the trend line $k_0 = 2.48(A_{13})^{-0.45}$.

power law of the structure factor is a function of shape anisotropy as well. In particular Eq. (15) for $D_f = 1.8$ and $\varphi = 0.68$ yields

$$S(q) = C(qR_g)^{-D_f} = \frac{1.35}{k_0}(qR_g)^{-D_f} \tag{21}$$

This equation is tested in Fig. 5 where the structure factor of clusters in various anisotropy (A_{13}) ranges is explored. Aggregates with $N \geqslant 50$ were divided into groups according to A_{13} as was done above for Fig. 1. The structure factor for the clusters in each group were averaged and k_0 was found using Eq. (21). For all A_{13} ranges a fractal dimension of $D_f = 1.8$ accurately describes the data. The structure factors in Fig. 5 show, once again, an anticorrelation between A_{13} and k_0 quantitatively consistent with that found in the real space analysis of Fig. 1 and our previous results [12]. This is demonstrated in Fig. 6. A fit to all the individual clusters yields a quantitative description of this anticorrelation that can be best described as

Please cite this article in press as: W.R. Heinson et al., J. Colloid Interface Sci. (2012), doi:10.1016/j.jcis.2012.01.062

$$k_0 = 2.48(A_{13})^{-0.45} \quad (22)$$

The system average prefactor was measured to be $\langle k_0 \rangle = 1.35$, hence the coefficient $C = 1.00$, as found previously [14]. Given this average prefactor, $D_f = 1.80$ and $\varphi = 0.68$, Eq. (11) yields $\langle \gamma \rangle = 2.02$, a value consistent with previous results [4,8]. From Eqs. (11) and (22) or equivalently the solid line in Fig. 3, $\langle A_{13} \rangle = 3.86$.

6. Discussion and conclusions

Numerous experimental studies of aggregates formed via DLCA have consistently found fractal dimensions of about 1.8 [1,3], in agreement with the simulations presented here and many previous simulations [2,5–9]. On the other hand prefactors and shape have been measured less frequently. The only experimental prefactor work of which we are aware is for carbonaceous soot in flames which has been shown to have a fractal structure with dimensions on the order of 1.8 but with prefactors ranging from $k_0 = 1.23$ to well over 2 [15–17]. Unlike the idealized point contacting spheres of simulation, however, soot can show significant "necking" between connecting monomers. It has been proposed that this necking or overlap is the reason for some of the soot prefactors to be larger than those of DLCA simulations [17,18]. One possible patch to the theory here would be to try to quantify monomer overlap with a variable packing fraction φ. Then via Eq. (11) k_0 could be made bigger. At this time, however, we are uncertain how to quantify overlap and justify its use in Eq. (3). Finally, we know of no work to measure fractal aggregate shape.

The theoretical work presented here reaffirms that an adequate description of the morphology of a fractal aggregate is contained in the pair D_f and k_0. The fractal dimension D_f describes the scaling of mass with linear dimension and the prefactor k_0 contains aggregate shape information. However, we find that a more fundamental and perhaps more complete description of morphology lies with the three parameters fractal dimension, D_f, the monomer pair correlation function stretching exponent, γ, and the monomer packing fraction, φ. The fractal prefactor k_0 is a function of these three parameters via Eq. (11). The aggregate anisotropy A_{13} is directly related to the stretching exponent γ and thus an equivalent descriptor. We found that the packing fraction, like the fractal dimension, was constant. But it would seem to be wise to be wary that it, like the fractal dimension, might be a function of the aggregation mechanism, such as RLCA or BLCA, monomer overlap or, in simulations, whether the process is performed on or off lattice. These questions open avenues for future study. In addition, we have focused here only on irreversible aggregation with an infinitely deep potential well describing the monomer–monomer interactions. For short-ranged potentials with a finite but deep well, one can have a hybrid structure of fractal morphology ("fat fractals") [19] leading to a different set of D_f, γ and φ. Finally, this work illustrates the effects of shape on both real space analysis, involved in the application of Eq. (1), and reciprocal space analysis via the structure factor.

Acknowledgments

One of us (CMS) has benefitted greatly from discussions with Don Holve of Process Metrix. This work was supported by the Kansas State University Target Excellence program.

References

[1] R. Jullien, R. Botet, Aggregation and Fractal Aggregates, World Scientific, Singapore, 1987.
[2] P. Meakin, Adv. Colloid Interf. Sci. 28 (1988) 249–331.
[3] M.Y. Lin, H.M. Lindsay, D.A. Weitz, R.C. Ball, R. Klein, P. Meakin, Nature 339 (1989) 360–363.
[4] C.M. Sorensen, Aerosol Sci. Technol. 35 (2001) 648–687.
[5] M. Kolb, R. Botet, R. Jullien, Phys. Rev. Lett. 51 (1983) 1123–1126.
[6] P. Meakin, Phys. Rev. Lett. 51 (1983) 1119–1122.
[7] C.M. Sorensen, G.C. Roberts, J. Colloid Interf. Sci. 186 (1997) 447–452.
[8] M. Lattuada, H. Wu, M. Morbidelli, J. Colloid Interf. Sci. 268 (2003) 96–105.
[9] F. Pierce, C.M. Sorensen, A. Chakrabarti, Phys. Rev. E 74 (2006) 021411.
[10] C.M. Sorensen, C. Oh, Phys. Rev. E 58 (1998) 7545–7548.
[11] D. Fry, A. Mohammed, A. Chakrabarti, C.M. Sorensen, Langmuir 20 (2004) 7871–7879.
[12] W.R. Heinson, C.M. Sorensen, A. Chakrabarti, Aerosol Sci. Technol. 44 (2010) i–iv.
[13] T. Nicolai, D. Durand, J.-C. Gimel, Phys. Rev. B 50 (1994) 16357–16363.
[14] C.M. Sorensen, G.M. Wang, Phys. Rev. E 60 (1999) 7143–7148.
[15] J. Cai, N. Lu, C.M. Sorensen, J. Colloid Interf. Sci. 171 (1995) 470–473.
[16] U.O. Koylu, G.M. Faeth, T.L. Farias, M.G. Carvalho, Combust. Flame 100 (1995) 621–633.
[17] A.M. Brasil, T.L. Farias, M.G. Carvalho, Aerosol Sci. Technol. 33 (2000) 440–454.
[18] C. Oh, C.M. Sorensen, J. Colloid Interf. Sci. 193 (1997) 17–25.
[19] A. Chakrabarti, D. Fry, C.M. Sorensen, Phys. Rev. E 69 (2004) 031408.